



# Interplay between autophagy and CncC regulates dendrite pruning in *Drosophila*

Jue Yu Kelly Tan<sup>a,b,1</sup>, Liang Yuh Chew<sup>a,b,1</sup> , Gábor Juhász<sup>c,d</sup>, and Fengwei Yu<sup>a,b,2</sup>

Edited by Hugo Bellen, Baylor College of Medicine, Houston, TX; received July 2, 2023; accepted January 26, 2024

Autophagy is essential for the turnover of damaged organelles and long-lived proteins. It is responsible for many biological processes such as maintaining brain functions and aging. Impaired autophagy is often linked to neurodevelopmental and neurodegenerative diseases in humans. However, the role of autophagy in neuronal pruning during development remains poorly understood. Here, we report that autophagy regulates dendrite-specific pruning of ddaC sensory neurons in parallel to local caspase activation. Impaired autophagy causes the formation of ubiquitinated protein aggregates in ddaC neurons, dependent on the autophagic receptor Ref(2)P. Furthermore, the metabolic regulator AMP-activated protein kinase and the insulin–target of rapamycin pathway act upstream to regulate autophagy during dendrite pruning. Importantly, autophagy is required to activate the transcription factor CncC (Cap “n” collar isoform C), thereby promoting dendrite pruning. Conversely, CncC also indirectly affects autophagic activity via proteasomal degradation, as impaired CncC results in the inhibition of autophagy through sequestration of Atg8a into ubiquitinated protein aggregates. Thus, this study demonstrates the important role of autophagy in activating CncC prior to dendrite pruning, and further reveals an interplay between autophagy and CncC in neuronal pruning.

autophagy | Atg8a | dendrite pruning | metamorphosis | CncC

To establish precise and functional neural circuits, neurons are constantly remodeled over the lifespan (1). During development, neurons often extend supernumerary projections at an earlier stage and subsequently remove aberrant or excessive projections without undergoing neuronal cell death, a process known as neuronal pruning (2). Neuronal pruning refines overabundant neuronal connections to establish mature nervous systems (3, 4). Classic examples of neuronal pruning in vertebrates include axonal pruning in layer V sub-cortical pyramidal neurons (5) and motoneuron axonal retraction at the neuromuscular junctions (6). Dysregulation in neuronal pruning is implicated in many neurodevelopmental disorders, such as autism spectrum disorders (ASDs), schizophrenia, and epilepsy (7, 8).

In *Drosophila*, neuronal pruning takes place during metamorphosis (9, 10). Two representative models are dendrite-specific pruning of dendritic arborization (da) sensory neurons in the peripheral nervous system (PNS) and axon pruning of mushroom body (MB)  $\gamma$  neurons in the central nervous system (CNS) (4). In the PNS, class II and class III da neurons are apoptotic, whereas class I and class IV da neurons survive but undergo dendrite-specific pruning (11, 12). ddaC neurons, a subset of dorsal class IV da neurons (C4da neurons), selectively prune their larval dendrites without affecting their axons. Dendrite pruning of ddaC neurons initiates with the occurrence of thinning and blebbing along proximal branches around 3 h after puparium formation (APF), followed by severing of proximal dendrites around 5 to 8 h APF. Severed dendrites are rapidly fragmented around 10 to 12 h APF and eventually cleared by phagocytes such as epidermal cells by 16 h APF (12–14). This stereotyped pruning event is triggered by a late larval pulse of the steroid hormone 20-hydroxyecdysone (ecdysone). Upon binding to ecdysone hormone, the heterodimeric nuclear receptor complex, namely ecdysone receptor–Ultraspiracle (EcR–Usp), activates its downstream signaling cascades (15), including the transcription factor Sox14 (13, 16) and a cytosolic protein Headcase (17). Sox14 further activates expression of the F-actin dismantling factor Mical (13).

We have recently demonstrated that ecdysone signaling is necessary and sufficient to activate the transcription factor Cap “n” collar isoform C (CncC), which plays a crucial role in dendrite pruning (18). In *Drosophila*, CncC was initially identified as a homolog of mammalian Nrf2 to regulate oxidative stress tolerance and lifespan (19). Nrf2 and its repressor Keap1 mediate a conserved stress response pathway that protects cells against oxidative and xenobiotic stresses (20, 21). Under normal conditions, Nrf2 is ubiquitinated by the Keap1-containing ubiquitin E3 ligase and rapidly degraded by proteasomes. Under

## Significance

Autophagy clears damaged organelles and long-lived proteins in eukaryotic cells including neurons. However, whether and how autophagy regulates elimination of neuronal processes during development remain poorly understood. Here, we report an important role of autophagy in regulating elimination of the dendrites of sensory neurons during *Drosophila* metamorphosis. We found that autophagy acts downstream of AMP-activated protein kinase and insulin–target of rapamycin pathway to regulate protein turnover in sensory neurons. Importantly, autophagy regulates activation of the transcription factor CncC (Cap “n” collar isoform C) prior to dendrite pruning. Conversely, CncC also modulates autophagic activity through sequestration of a key autophagic regulator. Thus, this study reveals an interplay between autophagy and CncC in neuronal pruning.

Author contributions: J.Y.K.T., L.Y.C., and F.Y. designed research; J.Y.K.T. and L.Y.C. performed research; J.Y.K.T., L.Y.C., and G.J. contributed new reagents/analytic tools; J.Y.K.T., L.Y.C., G.J., and F.Y. analyzed data; and J.Y.K.T., L.Y.C., and F.Y. wrote the paper.

The authors declare no competing interest.

This article is a PNAS Direct Submission.

Copyright © 2024 the Author(s). Published by PNAS. This article is distributed under [Creative Commons Attribution-NonCommercial-NoDerivatives License 4.0 \(CC BY-NC-ND\)](https://creativecommons.org/licenses/by-nc-nd/4.0/).

<sup>1</sup>J.Y.K.T. and L.Y.C. contributed equally to this work.

<sup>2</sup>To whom correspondence may be addressed. Email: fengwei@tli.org.sg.

This article contains supporting information online at <https://www.pnas.org/lookup/suppl/doi:10.1073/pnas.2310740121/-/DCSupplemental>.

Published February 26, 2024.

oxidative stress, Keap1 becomes inactivated, leading to stabilization of Nrf2. Nrf2 is subsequently translocated into the nucleus where it induces the transcription of cytoprotective targets against stress. In *Drosophila*, CncC also forms a protein complex with fly Keap1 via their conserved domains (22). Fly CncC is homologous not only to Nrf2 but also to another mammalian paralog Nrf1 (23). Growing evidence shows that Nrf1 induces compensatory upregulation of proteasomal subunits and activity upon proteasome inhibition (24–26). Like its mammalian counterparts, CncC translocates from the cytoplasm to the nucleus in ddaC neurons, which depends on ecdysone signaling (18). In the ddaC nuclei, CncC induces proteasomal subunit expression, thereby enhancing proteasomal degradation activity to promote dendrite pruning (18). On the other hand, ecdysone signaling modulates metabolic changes by inhibiting the insulin–target of rapamycin (TOR) pathway (27) and activating the energy sensor AMP-activated protein kinase (AMPK) (28, 29). AMPK acts upstream of the insulin–TOR pathway to activate CncC before dendrite pruning (29). Therefore, metabolic changes cause activation of CncC during the nonfeeding prepupal stages. However, how these metabolic changes activate CncC remains elusive.

Autophagy is a conserved catabolic process that delivers damaged or obsolete organelles and cytoplasmic proteins to lysosomes for degradation (30). Under nutrient deprivation, AMPK activity is elevated, and TOR is downregulated, which leads to Atg1 activation and autophagy induction. Upon induction of autophagy, a phagophore (also known as an isolation membrane) first forms around cytoplasmic components. It subsequently elongates and matures into a double-membrane autophagosome, which requires the Atg8 (also known as LC3 in mammals) and Atg5–Atg12 conjugation systems. Autophagosomes then fuse with lysosomes to degrade their contents for recycling (30). Impaired autophagy is linked to age-dependent neurodegenerative diseases as well as neurodevelopmental disorders in humans (31, 32). In *Drosophila*, autophagy is highly activated during metamorphosis, a developmentally programmed starvation period (33, 34). It mediates degradation of cytoplasmic proteins/organelles and even unwanted tissues (such as the larval fat body, salivary gland, or midgut) to recycle proteins and lipids for the development of adult-specific organs. While autophagy plays an important role in synapse formation and brain aging in *Drosophila* (35–37), it is dispensable for axonal pruning of MB  $\gamma$  neurons in the CNS (38). In this study, we identify autophagy as an important regulator of dendrite pruning. Moreover, autophagy is required for activation of CncC. Interestingly, CncC also modulates autophagy in ddaC neurons. We show that CncC impairment downregulates autophagic activity through sequestration of Atg8a. Thus, our study highlights an interplay between autophagy and CncC during neuronal pruning.

## Results

### Autophagy Is Required for Dendrite Pruning in ddaC Neurons.

The previous studies demonstrate that ecdysone signaling promotes dendrite pruning by inhibiting the insulin–TOR pathway and activating the energy sensor AMPK (27–29). Moreover, AMPK acts to inhibit the insulin–TOR pathway to govern dendrite pruning (29). Given that both AMPK and TOR govern autophagy induction under starvation (39–41), we attempted to assess a potential role of autophagy in dendrite pruning. To this end, we focused on several key autophagy regulators, such as Atg1, Atg5, and Atg8a. Interestingly, the expression of either of two independent *Atg1* RNAi constructs, via the class IV da-specific *ppk-Gal4* driver, led to consistent dendrite pruning defects in ddaC neurons at 16 h

APF (Fig. 1 *B, C, K, and L*). In contrast, the control RNAi neurons eliminated their larval dendrites at the same stage (Fig. 1 *A, K, and L*). Likewise, knockdown of *Atg8a* (RNAi #1 and #2) also significantly inhibited dendrite pruning in ddaC neurons (Fig. 1 *D, E, K, and L*). To verify these RNAi results, two *Atg8a* loss-of-function mutants, *Atg8a<sup>Δ4</sup>* (42) and *Atg8a<sup>KG07569</sup>* (43), were utilized to confirm its important role in dendrite pruning. Both *Atg8a<sup>Δ4</sup>* and *Atg8a<sup>KG07569</sup>* mutants displayed similar pruning defects in ddaC neurons at 16 h APF (Fig. 1 *F, G, K, and L*). Importantly, by using a transgene that expresses 3XmCherry-tagged *Atg8a* under the control of its endogenous promoter (*3XmCherry-Atg8a*) (44), we significantly rescued the pruning defects in *Atg8a<sup>KG07569</sup>* mutant ddaC neurons (Fig. 1 *H, K, and L*), confirming that loss of *Atg8a* function is responsible for the dendrite pruning defects in these mutant neurons. Lipidation of *Atg8a* is required for its covalent attachment to autophagosomes, a prerequisite step for elongation of phagophores, autophagosome closure, and autophagosome–lysosome fusion (45). Mutant ddaC neurons, derived from a non-lipidatable *Atg8a<sup>G116\*</sup>* allele (46), failed to prune away their dendrites by 16 h APF (Fig. 1 *I, K, and L*), compared to the wild-type neurons (Fig. 1 *K and L*). Moreover, ddaC neurons derived from the *Atg5<sup>5CC5</sup>* null mutant also exhibited dendrite pruning defects at 16 h APF (Fig. 1 *J, K, and L*). Collectively, our data demonstrate the important role of these key autophagy-related genes for dendrite pruning, suggesting that autophagy is required for dendrite pruning in ddaC sensory neurons.

### Autophagy Regulates Dendrite Pruning in Parallel to Local Caspase Activation.

During metamorphosis, autophagic degradation and caspases function independently to mediate the clearance of salivary glands (47, 48). However, midgut cells require autophagy but not caspases for their removal (49). In ddaC neurons, dendrite pruning requires activation of caspases that is locally restricted to the dendrites (50, 51). To examine whether local caspase activation is regulated by autophagy, we took advantage of the caspase reporter CD8::poly-ADP-ribose polymerase-1 (PARP)::Venus containing the caspase substrate PARP that can be cleaved by effector caspases (51). Cleaved PARP leads to exposure of the terminal cleavage site that can be recognized by a highly specific antibody. In the control ddaC neurons, activation of the CD8::PARP::Venus reporter was observed in the fragmenting dendrites that had been severed from the soma (*SI Appendix, Fig. S1A*). Similarly, activation of the reporter also occurred in the dendrites of *Atg1* or *Atg8a* RNAi neurons (*SI Appendix, Fig. S1 B and C*), suggesting that caspases are locally activated in these mutant neurons. Unlike ddaC neurons, the class III ddaF neuron is removed via apoptosis during metamorphosis (51). We observed the activation of the CD8::PARP::Venus reporter in the soma of *Atg1* or *Atg8a* RNAi ddaF neurons (*SI Appendix, Fig. S1 E–G*), suggesting that autophagy is dispensable for ddaF apoptosis. To test whether both autophagy and caspase activation are required for dendrite pruning in ddaC neurons, we overexpressed p35, a baculoviral inhibitor of effector caspases, or DIAP1, an E3 ubiquitin ligase with caspase inhibitor activity, in autophagy-deficient neurons to assess their effects on dendrite pruning. Notably, overexpression of p35 or DIAP1 in *Atg1* or *Atg8a* RNAi neurons exhibited stronger dendrite pruning defects (Fig. 2 *A and B*), compared to *Atg1* RNAi, *Atg8a* RNAi, p35 overexpression or DIAP1 overexpression alone (Fig. 2 *A and B*). Therefore, these data demonstrate that autophagy and caspase activation function in separate pathways to promote dendrite pruning.

**Impaired Autophagy Results in Robust Accumulation of Polyubiquitinated Protein Aggregates in ddaC Neurons.** We next investigated whether autophagy is important for clearance

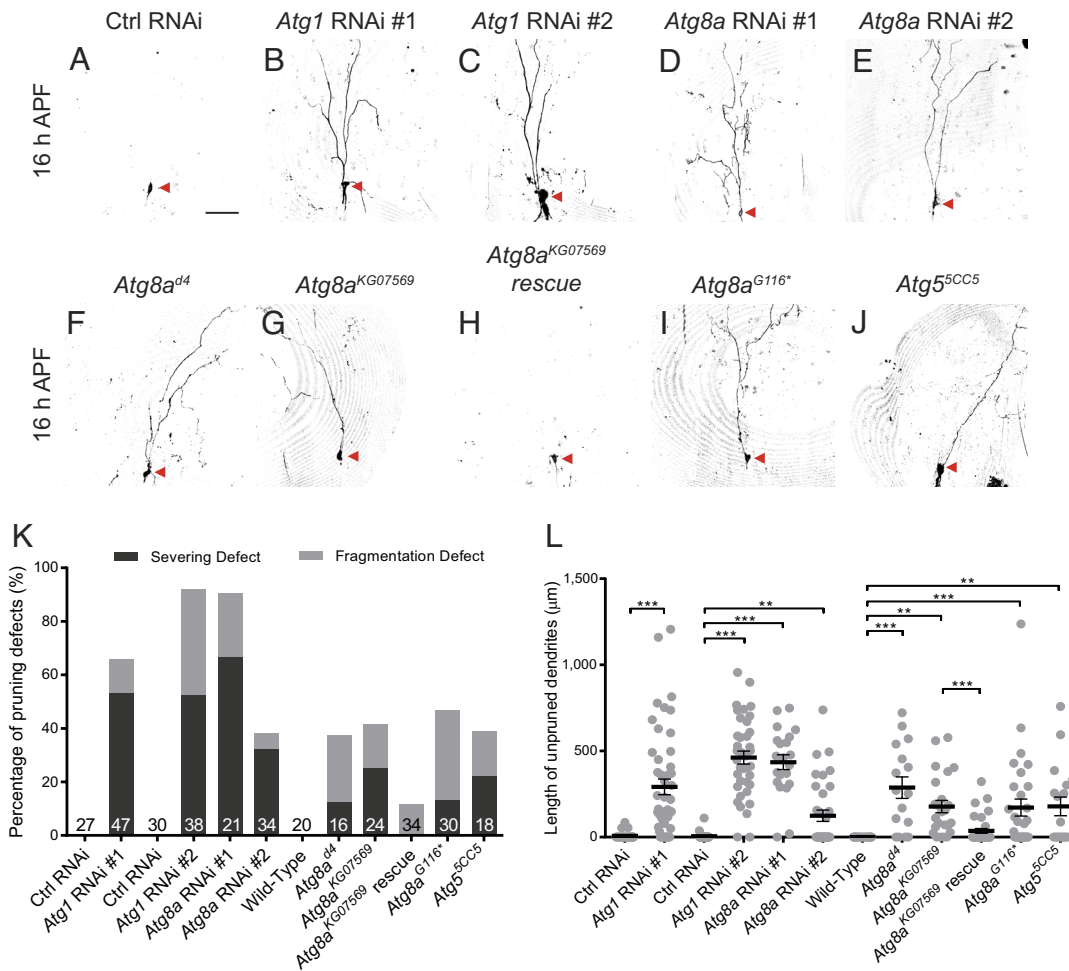


**Fig. 1.** Autophagy is required for dendrite pruning in ddaC neurons. (A–J) Representative live confocal images of ddaC neurons at 16 h APF. Dendrites of control RNAi (A), *Atg1* RNAi #1 (B), *Atg1* RNAi #2 (C), *Atg8a* RNAi #1 (D), *Atg8a* RNAi #2 (E), *Atg8a<sup>d4</sup>* (F), *Atg8a<sup>KG07569</sup>* (G), *Atg8a<sup>KG07569</sup>* rescue (H), *Atg8a<sup>G116\*</sup>* (I), *Atg5<sup>5CC5</sup>* (J) at 16 h APF. The ddaC soma is indicated with a red arrowhead. Quantitative analyses of percentage of pruning defects (K) and unpruned dendrite length (L) at 16 h APF. Error bars represent  $\pm$  SEM. The number of neurons (n) for each group is indicated above the x-axis. Statistical significance was assessed using a two-tailed Student's t test (\*\* $P < 0.01$ ; \*\*\* $P < 0.001$ ). The scale bar in (A) represents 50  $\mu$ m.

of unwanted protein substrates in ddaC neurons. The autophagic receptor p62, whose fly homolog is Ref(2)P (Refractory to sigma P), targets polyubiquitinated protein aggregates for autophagic degradation and thus is used as a readout to detect autophagy (42, 52–54). We thus measured Ref(2)P levels and distributions in autophagy-deficient ddaC neurons. As expected, knockdown of *Atg1* (RNAi #1 and #2) or *Atg8a* (RNAi #1 and #2) resulted in robust accumulation of large Ref(2)P puncta that overlapped with ubiquitinated protein aggregates (Fig. 3A and *SI Appendix, Table S1*), compared to no apparent protein aggregates in the control RNAi neurons. The total levels of Ref(2)P proteins were significantly elevated in *Atg1* or *Atg8a* RNAi neurons (Fig. 3A). The punctate signals are specific to Ref(2)P as they were eliminated when *ref(2)P* was knocked down in *Atg1* or *Atg8a* RNAi ddaC neurons (Fig. 4A and B). Similar to the RNAi knockdowns, *Atg8a<sup>d4</sup>*, *Atg8a<sup>KG07569</sup>*, and *Atg5<sup>5CC5</sup>* mutant ddaC neurons also exhibited prominent accumulation of Ref(2)P-positive ubiquitinated protein aggregates (Fig. 3A). The Ref(2)P-ubiquitin protein aggregation phenotype in *Atg8a<sup>KG07569</sup>* neurons was significantly rescued by the expression of 3XmCherry-Atg8a under the endogenous *Atg8a* promoter (*SI Appendix, Fig. S2A*). Moreover, the puncta size and number were also significantly increased in *Atg1/Atg8a* RNAi or mutant neurons (*SI Appendix, Table S2*). The ubiquitinated protein aggregates in *Atg1* RNAi or *Atg8a* RNAi neurons did not colocalize with the early and late endosomal/lysosomal markers FYVE-green fluorescent protein (GFP) and LAMP1-GFP, respectively (*SI Appendix, Fig. S2B and C and Table S1*), suggesting that these

protein aggregates reside in the cytosol. We next made use of the autophagosome marker mCherry-Atg8a (55). Compared to a lack of mCherry-Atg8a puncta in the control neurons, large and discrete mCherry-Atg8a punctate structures were present in *Atg1* RNAi neurons (Fig. 3B). These mCherry-Atg8a puncta colocalized with the ubiquitinated protein aggregates (Fig. 3B), indicating that Atg1 is required for the clearance of ubiquitinated proteins in ddaC neurons.

For autophagic degradation to occur, autophagosomes carrying ubiquitinated proteins fuse with acidic lysosomes to form autolysosomes. We made use of the dual fluorescent marker GFP-mCherry-Atg8a (56, 57) to assess autophagic flux. Upon autophagosome-lysosome fusion, the GFP fluorescence is quenched by the low pH in acidic autolysosomes but the mCherry fluorescence remains intact. In the soma of control neurons, all the puncta were mCherry-positive but GFP-negative autolysosomes (Fig. 3C). Interestingly, the GFP-mCherry-Atg8a reporter is both GFP-positive and mCherry-positive in *Atg1* RNAi neurons (Fig. 3C), suggesting that autophagic flux is inhibited in the absence of *Atg1*. Consistently, the ubiquitinated protein aggregates did not overlap with lysosomal markers (LAMP1-GFP and LysoTracker) in *Atg1* or *Atg8a* RNAi neurons (*SI Appendix, Fig. S2C and D*), indicating that these punctate structures are not autolysosomes. Moreover, those protein aggregates in *Atg1* or *Atg8a* RNAi neurons were negative for other early autophagic markers, such as GFP-Atg5 (Fig. 3D and E), Myc-Atg6 (*SI Appendix, Fig. S2E*) and GFP-Atg9 (*SI Appendix, Fig. S2F*). Thus, multiple lines of evidence suggest that the Ref(2)P-positive puncta are not autophagosome-related

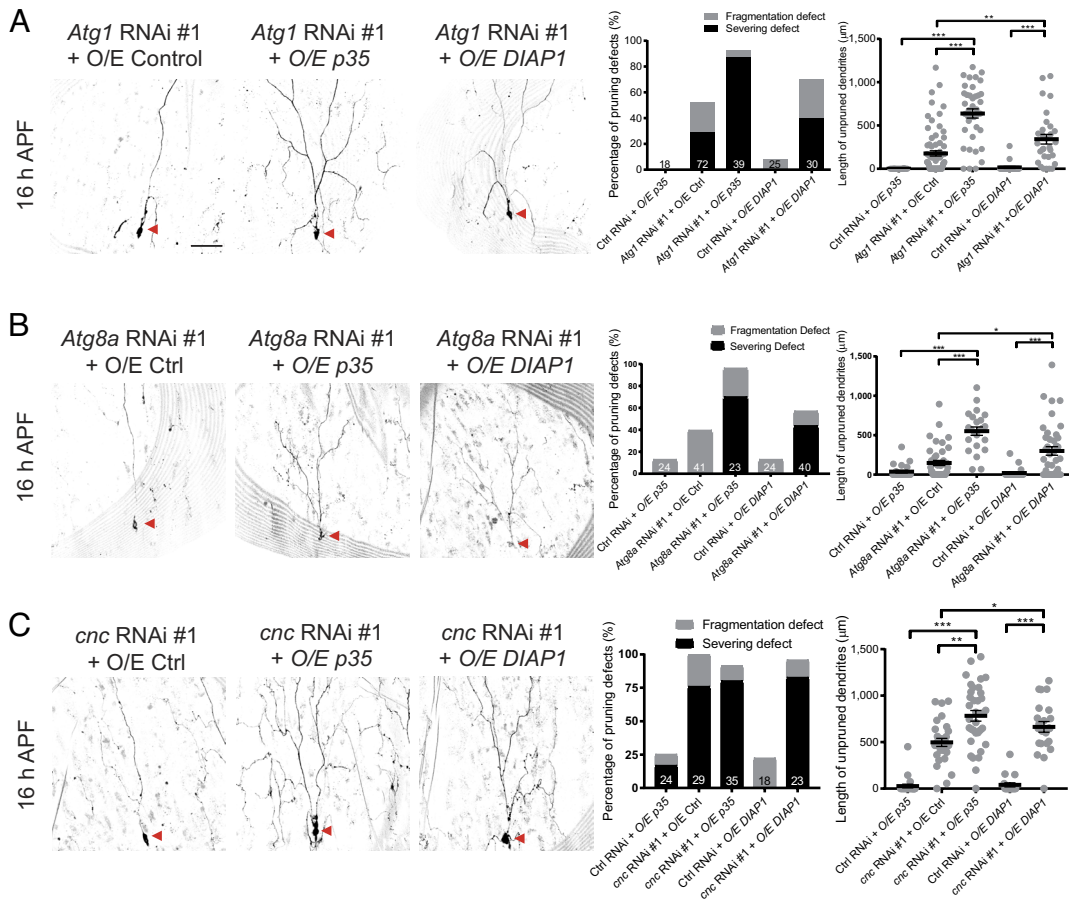


**Fig. 2.** Autophagy regulates dendrite pruning in parallel to local caspase activation. (A–C) Dendrites of *Atg1* RNAi #1 (A), *Atg8a* RNAi #1 (B) or *cnc* RNAi #1 (C) with control, *p35*, or *DIAP1* overexpressing *ddaC* neurons at 16 h APF. Red arrowheads indicate the soma. Quantitative analyses of percentage of pruning defects and unpruned dendrite length at 16 h APF are shown on the *Right* panels. Error bars represent  $\pm$  SEM. Statistical significance was assessed using One-way ANOVA with the Bonferroni test (\* $P < 0.05$ ; \*\* $P < 0.01$ ; \*\*\* $P < 0.001$ ). The number of neurons (*n*) examined is indicated above the *x*-axis. The scale bar in (A) represents 50  $\mu$ m.

structures but membrane-free protein aggregates (58). Taken together, our data demonstrate that autophagy is important for the clearance of ubiquitinated proteins in *ddaC* neurons.

**Ref(2)P Is Required for the Formation of Ubiquitinated Protein Aggregates and Contributes to the Dendrite Pruning Defects in *Atg1* or *Atg8a*-Depleted Neurons.** Ref(2)P and its mammalian homolog p62 bind to both cytosolic ubiquitinated proteins and autophagosomal Atg8a/LC3 to deliver ubiquitinated cargoes for autophagic-lysosomal degradation (52–54). To examine whether Ref(2)P contributes to the formation of ubiquitinated protein aggregates and the dendrite pruning defects associated with autophagy deficiency, we knocked down Ref(2)P in either *Atg1* (#1) or *Atg8a* (#1) RNAi *ddaC* neurons. In contrast to large ubiquitin-positive protein aggregates in *Atg1* or *Atg8a* single RNAi neurons, the aggregates were almost completely dispersed after further removal of Ref(2)P protein in these RNAi backgrounds (Fig. 4 *A* and *B*). The overall levels of ubiquitinated proteins in *Atg1-Ref(2)P* and *Atg8a-Ref(2)P* double RNAi neurons were significantly reduced (Fig. 4 *A* and *B*), compared to their respective controls. The reduction could be due to a compensatory increase in proteasomal degradation, as the proteasomal degradation reporter CL1-GFP was significantly downregulated in *Atg8a* RNAi neurons (SI Appendix, Fig. S2*G*). These data indicate that Ref(2)P is required for the formation of the protein aggregates in autophagy-deficient neurons. Moreover, knockdown of Ref(2)P ameliorated the dendrite pruning defects in *Atg1* or *Atg8a* RNAi neurons, as the unpruned dendrites were significantly reduced in length in *ref(2)P/Atg1* or *ref(2)P/Atg8a* double RNAi neurons (Fig. 4 *D* and *E*). Thus, Ref(2)P is required for the formation of ubiquitinated protein aggregates and in part contributes to

the dendrite pruning defects in *Atg1* or *Atg8a* RNAi neurons (SI Appendix, Discussion).

Autophagy is thought to recycle the unwanted proteins to maintain the pool of amino acids for protein synthesis and energy production during metamorphosis, a non-feeding stage (34). We next examined whether depriving the animals of amino acids can enhance the pruning defects in autophagy-deficient neurons. To do this, we altered the amino acid composition in fly food by controlling the yeast percentage (59, 60). Larvae were reared on a low yeast diet (LYD) containing 1.2% yeast without affecting pupal formation. We confirmed that the control animals reared on the LYD diet were able to completely prune larval dendrites of *ddaC* neurons by 16 h APF (SI Appendix, Fig. S3), similar to those on normal food diet containing 5% yeast (SI Appendix, Fig. S3). Interestingly, in *Atg1* or *Atg8a* RNAi animals raised on LYD, their *ddaC* neurons exhibited more severe pruning defects, compared to those derived from the normal food diet (SI Appendix, Fig. S3). Although the proteasomes remained active in autophagy-deficient neurons (SI Appendix, Fig. S2*G*), they were unable to degrade the Ref(2)P-containing ubiquitinated protein aggregates (Fig. 3*A*), which might cause an amino acid deficit. Thus, our data suggest that the LYD, which restricts the supply of amino acids, might further exacerbate the amino acid deficit, and thereby lead to even stronger pruning defects in autophagy-deficient neurons.

**AMPK and the Insulin-TOR Pathway Are Important for Autophagy in *ddaC* Neurons.** AMPK and the insulin-TOR pathway have been demonstrated to maintain energy level and regulate dendrite pruning in *ddaC* neurons (27–29). The insulin-TOR pathway has an inhibitory effect on autophagy whereas AMPK activates autophagy (39–41). We next assessed a possible role of AMPK and the insulin-TOR pathway in activating autophagy in *ddaC* neurons.

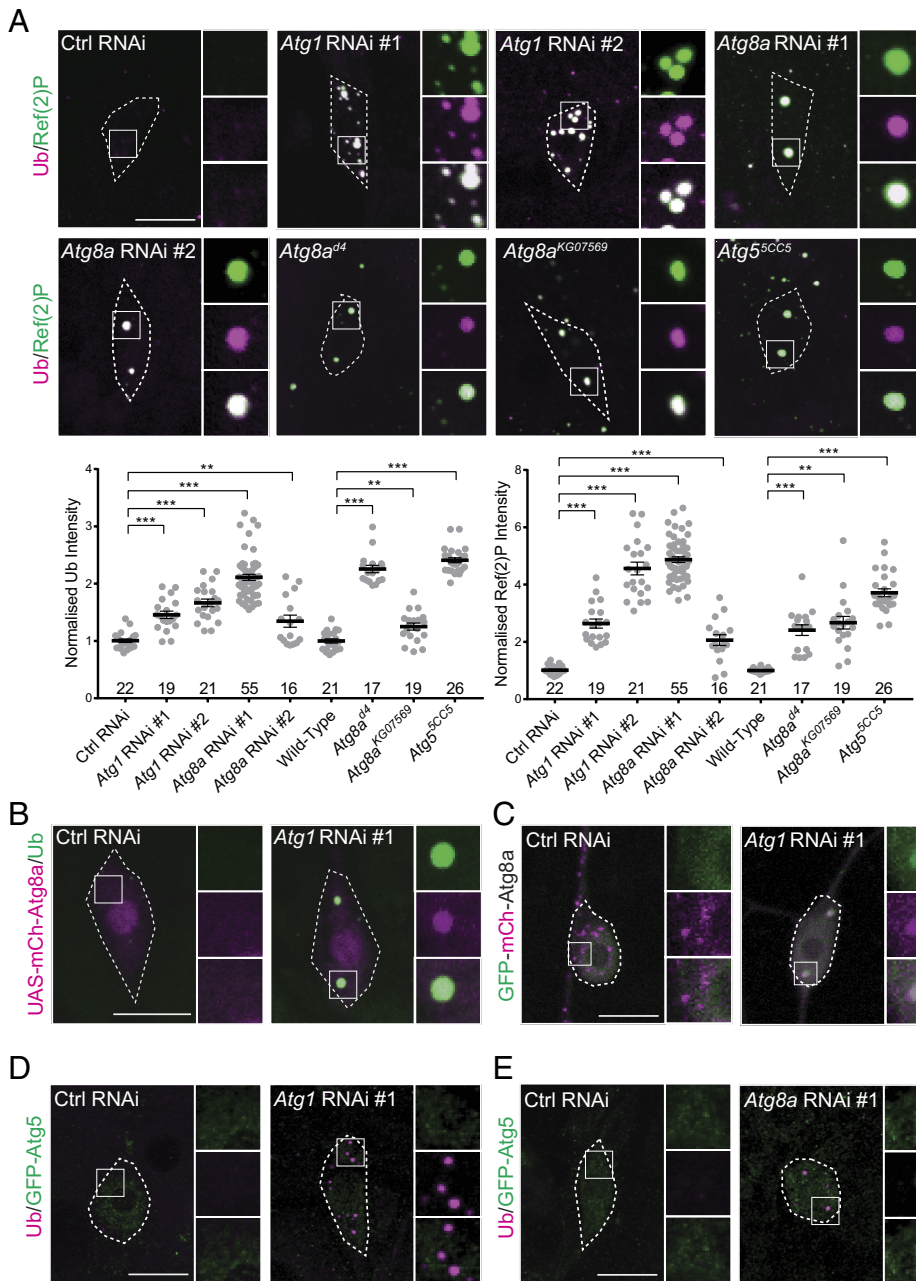


**Fig. 3.** Impaired autophagy resulted in robust accumulation of polyubiquitinated protein aggregates in ddaC neurons. (A) Expression of Ub and Ref(2)P in control RNAi, *Atg1* RNAi #1, *Atg1* RNAi #2, *Atg8a* RNAi #1, *Atg8a* RNAi #2, *Atg8a*<sup>d4</sup>, *Atg8a*<sup>KG07569</sup>, and *Atg5*<sup>5CC5</sup> ddaC neurons. Relevant quantifications of normalized Ub and Ref(2)P fluorescent intensities are shown on the *Bottom* panels. Error bars represent  $\pm$  SEM. Two-tailed Student's *t* test was used to determine statistical significance (\*\**P* < 0.01; \*\*\**P* < 0.001). The number of neurons (*n*) examined is indicated above the *x*-axis. (B) Expression of Ub in control RNAi (*n* = 25) or *Atg1* RNAi #1 (*n* = 23) ddaC neurons co-expressing *UAS-mCherry-Atg8a*. (C) Live images of control RNAi (*n* = 22), *Atg1* RNAi #1 (*n* = 17) ddaC neurons co-expressing the GFP-mCherry-*Atg8a* reporter. (D and E) Expression of Ub in control RNAi (*n* = 20), *Atg1* RNAi #1 (*n* = 18) (D) or *Atg8a* RNAi #1 (*n* = 12) (E) co-expressing the GFP-*Atg5* reporter. All specimens were observed at the late L3 stage. White dashed lines define the boundary of the ddaC somas. The boxed regions are magnified on the *Right* panels. Scale bar represent 10  $\mu$ m.

Interestingly, knockdown of AMPK $\alpha$  (called AMPK hereafter) (RNAi #1 and #2) led to significant accumulation of Ref(2)P/ubiquitinated protein aggregates in ddaC neurons (Fig. 5A and *SI Appendix, Table S1*). The level, size, and number of ubiquitin/Ref(2)P-positive puncta were significantly increased in these RNAi neurons (Fig. 5A and *SI Appendix, Table S2*), suggesting that autophagic degradation of Ref(2)P is compromised. Likewise, overexpression of InR<sup>CA</sup> (the constitutively active form of InR), Akt, and TOR, which leads to hyperactivation of the insulin-TOR pathway, also caused prominent accumulation of Ref(2)P-Ub-positive aggregates with TOR overexpression bearing the most robust accumulation (Fig. 5B and *SI Appendix, Fig. S4A* and *Table S2*). Furthermore, the ubiquitinated protein aggregates in *AMPK* RNAi, InR<sup>CA</sup>, or TOR-overexpressing neurons colocalized with mCherry-*Atg8a*-positive puncta (Fig. 5C and *SI Appendix, Table S1*), suggesting that AMPK and repression of the insulin-TOR pathway are required for autophagic degradation. Moreover, similar to those in *Atg1* or *Atg8a* RNAi neurons, the autophagic flux was suppressed in *AMPK* RNAi, InR<sup>CA</sup>- and TOR-overexpressing neurons as shown by the

increased number of mCherry-positive and GFP-positive punctate structures using the GFP-mCherry-*Atg8a* flux reporter (Fig. 5D). Of note, the ubiquitinated protein aggregates found in *AMPK* RNAi, InR<sup>CA</sup>- or TOR-overexpressing neurons did not colocalize with the lysosomal markers LAMP1-GFP (*SI Appendix, Fig. S4B* and *Table S1*) and LysoTracker (*SI Appendix, Fig. S4C* and *Table S1*). Moreover, the protein aggregates in *AMPK* RNAi neurons were not labeled by other early autophagic markers Myc-*Atg6* and GFP-*Atg9* (*SI Appendix, Fig. S4D* and *E*). Our data suggest that these protein aggregates are membrane-free structures, like those observed in *Atg1* or *Atg8a* RNAi neurons. AMPK knockdown and hyperactivation of the insulin-TOR pathway phenocopied *Atg1* or *Atg8a* knockdowns. Thus, these data suggest that AMPK and insulin-TOR pathway act upstream to regulate autophagy in ddaC neurons.

AMPK acts upstream to inhibit the insulin-TOR pathway to promote dendrite pruning (29), and inhibition of the insulin-TOR pathway is required for autophagy activation in ddaC neurons (Fig. 5C). We therefore hypothesized that the autophagy defects in *AMPK* RNAi neurons can be rescued by suppressing the

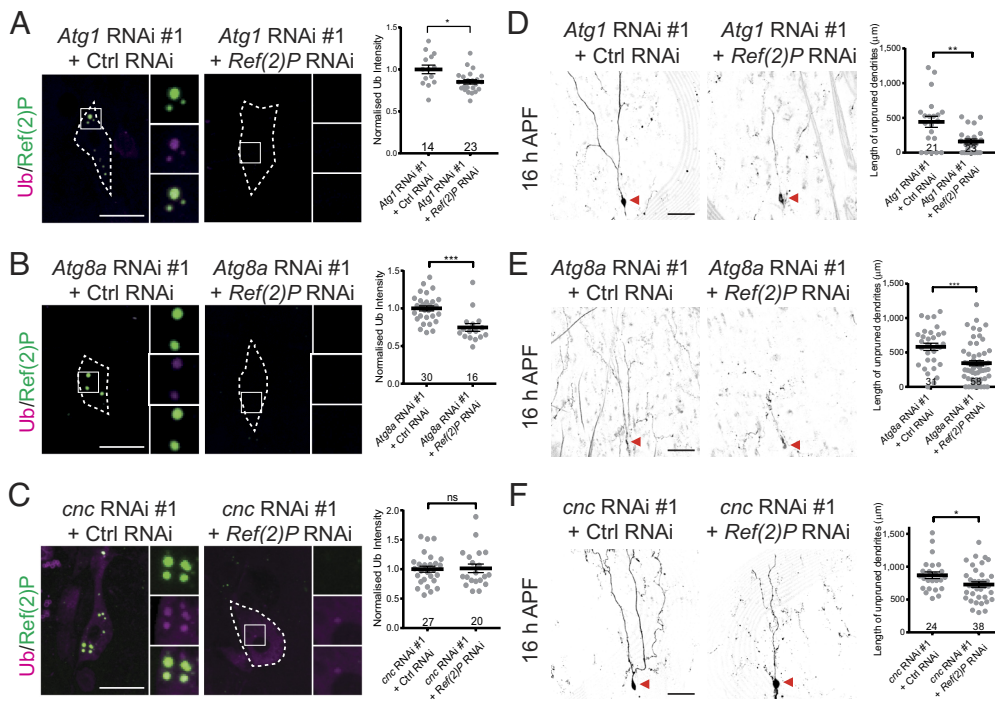


**Fig. 4.** Ref(2)P is required for the formation of protein aggregates and contributes partly to the dendrite pruning defects in *Atg1*- or *Atg8a*-deficient neurons. (A–C) Expression of Ub and Ref(2)P in *Atg1* RNAi #1 (A), *Atg8a* RNAi #1 (B), or *cnc* RNAi #1 (C) ddaC neurons co-expressing control RNAi or Ref(2)P RNAi at late L3 stage (n = 14 to 30). White dashed lines define the boundary of the ddaC somas. The boxed regions are magnified in the right panels. Relevant quantifications of normalized Ub fluorescent intensities are shown accordingly on the *Right* panels. (D–F) Dendrites of *Atg1* RNAi #1 (D), *Atg8a* RNAi #1 (E), or *cnc* RNAi #1 (F) ddaC neurons co-expressing control RNAi or Ref(2)P RNAi at 16 h APF. The ddaC soma is indicated with a red arrowhead. Quantitative analyses of unpruned dendrite length at 16 h APF are shown on the *Right* panels. Error bars represent  $\pm$  SEM. The number of neurons (n) for each group is indicated above the x-axis. Statistical significance was assessed using a two-tailed Student's *t* test (ns, non-significant; \**P* < 0.05; \*\**P* < 0.01; \*\*\**P* < 0.001). The scale bars in (A–C) and (D–F) represent 10  $\mu$ m and 50  $\mu$ m, respectively.

insulin–TOR pathway. Indeed, the Ref(2)P-ubiquitin-positive aggregates were gone when InR<sup>DN</sup>, *akt* RNAi, *TOR* RNAi, or TSC1–TSC2 (forming a negative regulator complex of TOR) was expressed in *AMPK* RNAi neurons (SI Appendix, Fig. S5 A and B), in contrast to the Ref(2)P-ubiquitin aggregates that robustly accumulated in *AMPK* RNAi neurons alone (SI Appendix, Fig. S5 A and B). As controls, the expression of InR<sup>DN</sup>, *akt* RNAi, *TOR* RNAi, or TSC1–TSC2 alone caused no accumulation of Ref(2)P-ubiquitin aggregates (SI Appendix, Fig. S5C). Thus, these data suggest that AMPK functions upstream to inhibit the insulin–TOR pathway and thereby activate autophagy in ddaC neurons.

Together with our previous findings (29), these data indicate that AMPK and the insulin–TOR pathway regulate ddaC dendrite pruning at least partly via activation of autophagy.

**Atg8a Is Required for CncC Activation Prior to Dendrite Pruning.** We next attempted to understand the mechanism of how autophagy regulates dendrite pruning. It has been reported that impaired autophagy causes sequestration of Keap1 into Ref(2)P/p62-positive ubiquitinated protein aggregates, leading to elevated CncC and Nrf2 activity in flies and mice, respectively (61, 62), suggesting that autophagy plays an inhibitory role in regulating CncC/Nrf2 activity. Moreover, CncC is activated by ecdysone signaling to govern dendrite pruning (18). We therefore investigated the possible role of *Atg8a* in activating CncC during dendrite pruning. We utilized two CncC readouts, namely *gstD1-lacZ* and *Rpn7* (18, 29), to assess the activity of CncC at 6 h APF, a stage before the onset of dendrite pruning. In the control RNAi ddaC neurons, *gstD1-lacZ* and *Rpn7* were expressed at 6 or 7 h APF (Fig. 6 A and B and SI Appendix, Fig. S6 B and D) but not at the wandering 3rd instar larval (wL3) stage (SI Appendix, Fig. S6 A and C), as reported in our previous findings (18, 29). Interestingly, *Atg8a* RNAi neurons displayed significant reductions in the levels of both *gstD-lacZ* and *Rpn7* at 6 h APF (Fig. 6 A and B). Consistent with these findings, both reporters were downregulated in *Atg8a*<sup>KG07569</sup> mutant neurons at 6 or 7 h APF (Fig. 6 A and B and SI Appendix, Fig. S6 B and D). As controls, these reporters remained silent in *Atg8a*<sup>KG07569</sup> mutant neurons at wL3 stage

(SI Appendix, Fig. S6 A and C), like wild-type neurons. These data indicate that impaired *Atg8a* function leads to inactivation of CncC in ddaC neurons during dendrite pruning. Since CncC is activated through its cytoplasmic-to-nuclear translocation (18), we then measured the nuclear levels of CncC at 6 or 7 h APF. Importantly, the nuclear levels of CncC were significantly decreased in *Atg8a* RNAi or *Atg8a*<sup>KG07569</sup> mutant neurons at 6 or 7 h APF (Fig. 6C and SI Appendix, Fig. S6F), compared to those in their respective control neurons. As a control, CncC was mainly localized in the cytoplasm of *Atg8a*<sup>KG07569</sup> mutant neurons at wL3 stage (SI Appendix, Fig. S6E), like that in the wild-type neurons. Taken together, these data strongly indicate that the CncC level/activity was reduced upon *Atg8a* depletion. Moreover, overexpression of CncC significantly enhanced the expression levels of *gstD1-lacZ* and *Rpn7* in *Atg8a*<sup>KG07569</sup> mutant neurons (SI Appendix, Fig. S7 A and B), strengthening the conclusion that *Atg8a* is required for CncC activation prior to dendrite pruning. In addition, we also overexpressed CncC or removed one copy of the *cncC* gene in *Atg8a* RNAi neurons to examine the genetic interaction between *cncC* and *Atg8a*. Interestingly, overexpression of CncC significantly suppressed the pruning defects in *Atg8a* RNAi neurons (Fig. 6D). Moreover, removal of one copy of the *cncC* gene strongly enhanced the dendrite pruning defects in *Atg8a* RNAi neurons (Fig. 6E). We observed no colocalization of either endogenous or overexpressed Keap1 proteins with ubiquitinated protein aggregates in *Atg8a* RNAi or *Atg8a*<sup>KG07569</sup> mutant neurons (SI Appendix, Fig. S5D). Thus, unlike mouse livers and fly adult brains (61, 62), ddaC neurons appeared to show no sequestration of Keap1 into the ubiquitinated protein aggregates when autophagy was impaired during the larval-to-pupal transition. Collectively, these data demonstrate that *Atg8a*-mediated autophagy is required for activation of CncC prior to dendrite pruning, contrasting to the inhibitory role of autophagy in other contexts (61, 62).

Taken together, our data suggest that AMPK and inactivation of the insulin–TOR pathway induce autophagy during the larval–pupal transition; autophagy in turn activates CncC to promote dendrite pruning in ddaC neurons.

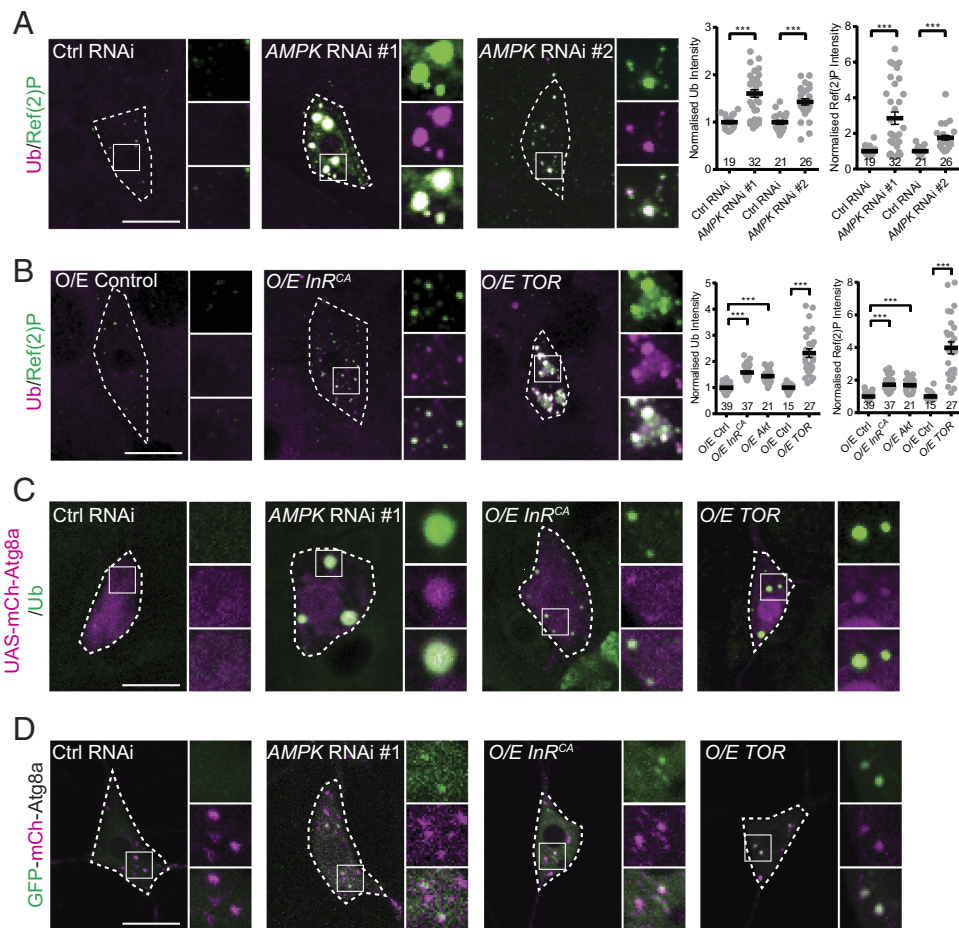


**Fig. 5.** AMPK and repression of the insulin-TOR pathway act upstream to activate autophagy in *ddaC* neurons. (A and B) Expression of Ub and Ref(2)P in *ddaC* neurons expressing control RNAi, AMPK RNAi #1, AMPK RNAi #2 (A), control, *InR<sup>CA</sup>* or TOR overexpression (B). (C) Expression of Ub in control RNAi ( $n = 12$ ), AMPK RNAi #1 ( $n = 20$ ), *InR<sup>CA</sup>* ( $n = 20$ ), or TOR ( $n = 18$ ) overexpressing *UAS-mCherry-Atg8a*. (D) Live images of control RNAi ( $n = 15$ ), AMPK RNAi #1 ( $n = 37$ ), *InR<sup>CA</sup>* ( $n = 15$ ), or TOR ( $n = 18$ ) overexpressing *ddaC* neurons co-expressing the GFP-mCherry-Atg8a reporter. All specimens were observed at the late L3 stage. White dashed lines define the boundary of the *ddaC* somas. The boxed regions are magnified on the *Right* panels. Relevant quantifications of normalized Ub and Ref(2)P fluorescent intensities are shown accordingly on the *Right*. Error bars represent  $\pm$  SEM. Statistical significance was assessed using a two-tailed Student's *t* test ( $***P < 0.001$ ). The number of neurons ( $n$ ) examined is indicated above the x-axis. Scale bar represent 10  $\mu$ m.

**Impaired CncC Results in the Inhibition of Autophagy in *ddaC* Neurons.** Autophagy genes (including *Atg8a*) and Ref(2)P/p62 have been reported to be transcriptional targets of CncC and Nrf2 in flies and mammals, respectively (22, 63, 64). We attempted to examine a possible existence of a positive feedback loop between autophagy and CncC in *ddaC* neurons. To test this possibility, we investigated whether CncC regulates autophagy in *ddaC* neurons by inducing Atg8a and Ref(2)P expression. Interestingly, knockdown of *cncC*, via two validated RNAi lines #1 and #2 (18), did not cause Ref(2)P downregulation, but instead resulted in robust accumulation of Ref(2)P protein on the ubiquitinated protein deposits as well as in the cytoplasm (Fig. 7A and *SI Appendix, Tables S1 and S2*). Furthermore, removal of Ref(2)P led to dispersal of the ubiquitinated protein puncta (Fig. 4C) and significantly suppressed the pruning defects in *cncC* RNAi neurons (Fig. 4F). Thus, Ref(2)P also controls the formation of protein inclusion bodies and contributes partly to the pruning defects in *cncC*-depleted *ddaC* neurons, similar to those in autophagy-deficient neurons (*SI Appendix, Discussion*).

The ubiquitinated protein aggregates in *cncC* RNAi neurons colocalized with mCherry-Atg8a-positive puncta (Fig. 7B). The autophagic flux was suppressed in *cncC* RNAi neurons, as all the GFP-mCherry-Atg8a puncta are mCherry-positive and GFP-positive in the mutant neurons (Fig. 7C), compared to mCherry-positive and GFP-negative puncta in the control neurons (Fig. 7C). In addition, in *cncC* RNAi neurons, the protein aggregates colocalized with neither the early endosomal marker FYVE-GFP (*SI Appendix, Fig. S8A*), the late endosomes GFP-Rab7 (*SI Appendix, Fig. S8B*), the recycling endosomes Rab11-GFP (*SI Appendix, Fig. S8C*), the late endosomal/lysosomal marker LAMP1-GFP (*SI Appendix, Fig. S8D*), nor the endoplasmic reticulum (ER) marker YFP-Rab1 (*SI Appendix, Fig. S8E*).

Importantly, the protein aggregates in *cncC* RNAi neurons were not labeled by other autophagic markers, such as Myc-Atg6 (*SI Appendix, Fig. S8F*) and GFP-Atg9 (*SI Appendix, Fig. S8G*), and the lysosomal marker LysoTracker (*SI Appendix, Fig. S8H*), suggesting that these protein puncta are membrane-free protein aggregates. In addition, the caspase reporter CD8::PARP::Venus was also activated in the dendrites of *cncC* RNAi neurons (*SI Appendix, Fig. S1D*) and *ddaF* soma (*SI Appendix, Fig. S1H*). Overexpression of p35 or DIAP1 enhanced the dendrite pruning defects in *cncC* RNAi neurons (Fig. 2C). Overall, all these *cncC* RNAi phenotypes are identical to those defects observed in *Atg1* or *Atg8a* RNAi neurons (Figs. 2 and 3 and *SI Appendix, Figs. S1 and S2*), suggesting that CncC is required for autophagic degradation. Taken together, these data indicate an interdependence between autophagy and CncC. While autophagy is required for activation of CncC prior to dendrite pruning, autophagy activity is also regulated by CncC.

We next explored how autophagy is regulated by CncC. Atg8a and Ref(2)P are potential transcriptional targets of CncC in the fly (22). However, Ref(2)P levels were elevated in *cncC* RNAi (Fig. 7A), suggesting that CncC is not required to induce Ref(2)P expression in *ddaC* neurons. Similar to Ref(2)P, we also observed an accumulation of endogenous Atg8a protein on the ubiquitinated protein aggregates in *cncC* RNAi neurons (Fig. 7D). These Atg8a fluorescence signals are specific, as they were depleted upon *cncC* and *Atg8a* double RNAi knockdown (*SI Appendix, Fig. S8I*). In addition, overexpression of CncC neither enhanced the expression of 3XmCherry-Atg8a protein which is under the control of its endogenous promoter nor affected Ref(2)P levels at the late 3rd instar larval (L3) or 6 h APF stages (*SI Appendix, Fig. S9A*). These data suggest that Ref(2)P and Atg8a are not transcriptional targets of CncC in *ddaC* neurons. Thus, CncC does not regulate autophagy through Ref(2)P and Atg8a expression

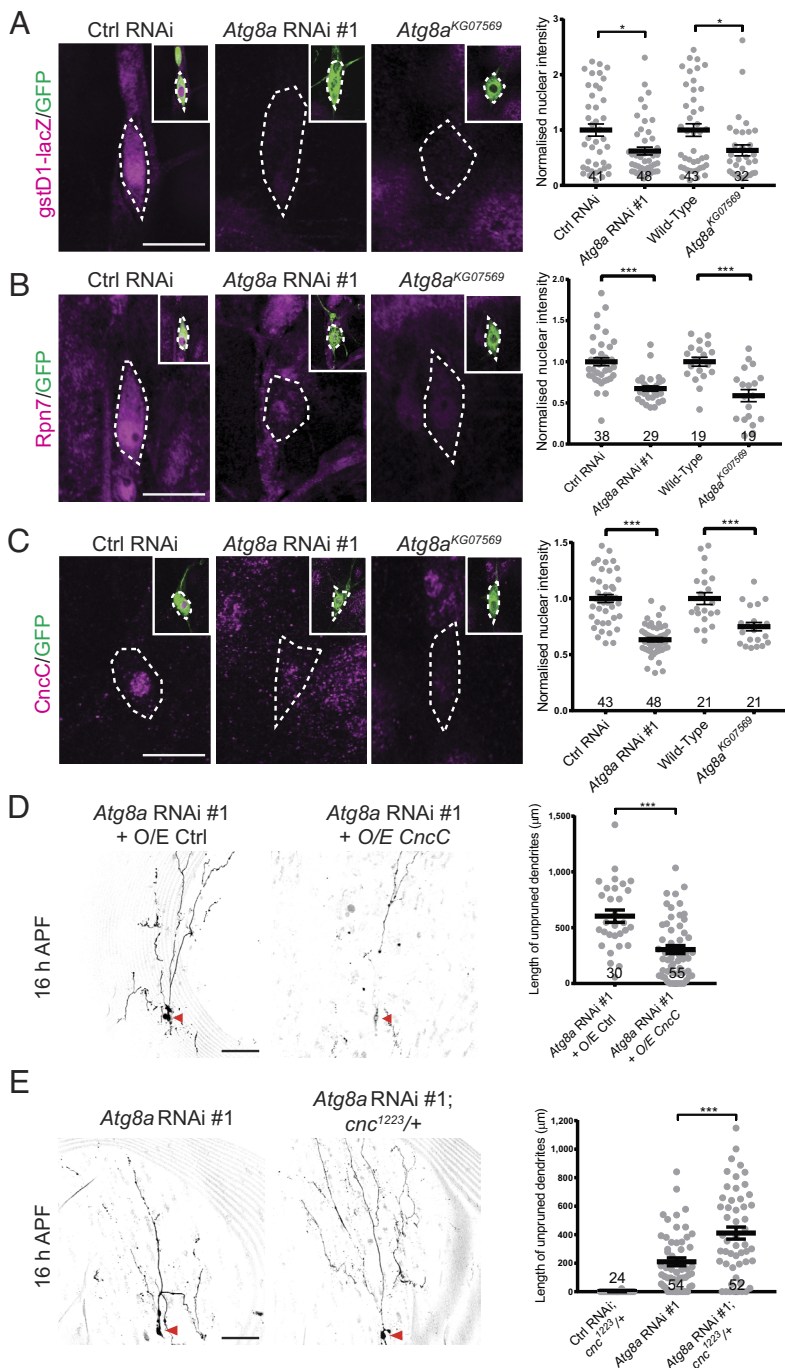


**Fig. 6.** *Atg8a* is required for activation of CncC prior to dendrite pruning. (A–C) Expression of *gstD1-lacZ* (A), Rpn7 (B) or CncC (C) in control RNAi, *Atg8a* RNAi #1 or *Atg8a*<sup>KG07569</sup> ddaC neurons. All specimens in (A–C) were dissected at 6 h APF. White dashed lines define the boundary of the ddaC somas. (D) Dendrites of *Atg8a* RNAi #1 ddaC neurons co-expressing control or *CncC* at 16 h APF. (E) Dendrites of *Atg8a* RNAi #1 or *Atg8a* RNAi #1 in *cnc*<sup>1223/+</sup> mutant background at 16 h APF. The ddaC soma is indicated with a red arrowhead. Quantitative analyses of normalized fluorescence intensities (A–C) or unpruned dendrite length (D and E) are shown on the *Right* panel. Error bars represent  $\pm$  SEM. The number of neurons (*n*) for each group is indicated above the *x*-axis. Statistical significance was assessed using a two-tailed Student's *t* test (\**P* < 0.01; \*\*\**P* < 0.001). The scale bars in (A–C) and (D and E) represent 10  $\mu$ m and 50  $\mu$ m, respectively.

in ddaC neurons. Interestingly, we observed even more robust Ref(2)P-positive ubiquitinated protein aggregates when the proteasomal subunit Mov34 (also known as Rpn8) was knocked down in ddaC neurons (*SI Appendix, Fig. S9B*), which was much more severe than *cnc* RNAi knockdown (Fig. 7A). Removal of Ref(2)P disrupted the formation of the protein aggregates (*SI Appendix, Fig. S9C*). The autophagosome markers (mCherry-Atg8a and GFP-mCherry-Atg8a) were enriched on the protein aggregates in *mov34* RNAi neurons (*SI Appendix, Fig. S9D and E*). Thus, the *cnc* mutant phenotypes, albeit weaker, are largely similar to *mov34* knockdown. These similar phenotypes can be explained by the role of CncC in proteasomal degradation, because CncC is able to induce proteasomal subunit transcription and hence enhance proteasomal degradation activity in ddaC neurons, as reported in our previous study (18).

We further examined how impaired proteasomal degradation in *cnc* RNAi ddaC neurons compromises autophagy. We proposed the possibility that through its direct interaction with Ref(2)P (22), endogenous Atg8a was captured into those Ref(2)P-positive ubiquitinated protein aggregates in *cnc* RNAi neurons (Fig. 7D), leading to sequestration of endogenous Atg8a protein and thereby impairment of autophagy. In line with this possibility, further removal of the *Atg8a* gene did not enhance the dendrite pruning defects in *cnc* RNAi neurons (*SI Appendix, Fig. S9F*), suggesting that Atg8a function is largely (if not completely) disrupted in *cnc* RNAi neurons. Thus, our data suggest that impaired CncC compromises the proteasomal degradation machinery and causes strong accumulation of ubiquitinated protein aggregates which can sequester endogenous Atg8a protein through its binding to Ref(2)P, thereby leading to inhibition of autophagy.



Taken together, we demonstrate that autophagy is required for activation of CncC; importantly, CncC also indirectly regulates autophagy activity via proteasomal degradation (SI Appendix, Fig. S10A). Our study reveals an interplay between autophagy and CncC that plays a pivotal role in dendrite pruning in ddaC neurons (SI Appendix, Fig. S10A).

## Discussion

**Autophagy Regulates Dendrite Pruning of ddaC Neurons Downstream of AMPK and Insulin-TOR Pathway.** Growing studies demonstrate that autophagy plays crucial roles in neuronal health and diseases (31, 32, 65). In *Drosophila*, autophagy has been shown to regulate neuronal development, aging, and injury (35, 66, 67). However, the role of autophagy in neuronal remodeling is less understood. In this study, we report an essential role of autophagy in regulating dendrite pruning of ddaC sensory neurons. Multiple lines of genetic evidence demonstrate that the key autophagy regulators, such as the autophagy initiation gene *Atg1* and two

autophagosome maturation genes *Atg5/Atg8a*, are required to regulate dendrite pruning in parallel to local caspase activation. Loss of these autophagy genes led to robust accumulation of ubiquitinated protein aggregates in ddaC neurons, similar to *Atg5* or *Atg7* mutant neurons in mice (68, 69). The ubiquitinated protein aggregates are positive for Ref(2)P, a key autophagic receptor. This suggests that autophagy-mediated protein degradation is disrupted in the absence of these autophagy genes. We further show that Ref(2)P is required for the formation of the ubiquitinated protein aggregates and in part for the dendrite pruning defects in autophagy-deficient neurons. In support of it, Ref(2)P and its mammalian homolog p62 are able to associate with poly-ubiquitinated proteins and also crosslink them via oligomerization (22, 70). In contrast to our present study, a previous study reported that autophagy is dispensable for axon pruning of MB  $\gamma$  neurons in CNS, as loss of *Atg1* or *Atg7* function did not show apparent pruning defects (38). Surprisingly, RNA profiling studies show that various autophagy regulators, including *Atg1*, *Atg5*, and *Atg8a*, are upregulated in an ecdysone-dependent manner in MB  $\gamma$  neurons from larva to pupa (71), similar to the upregulation of

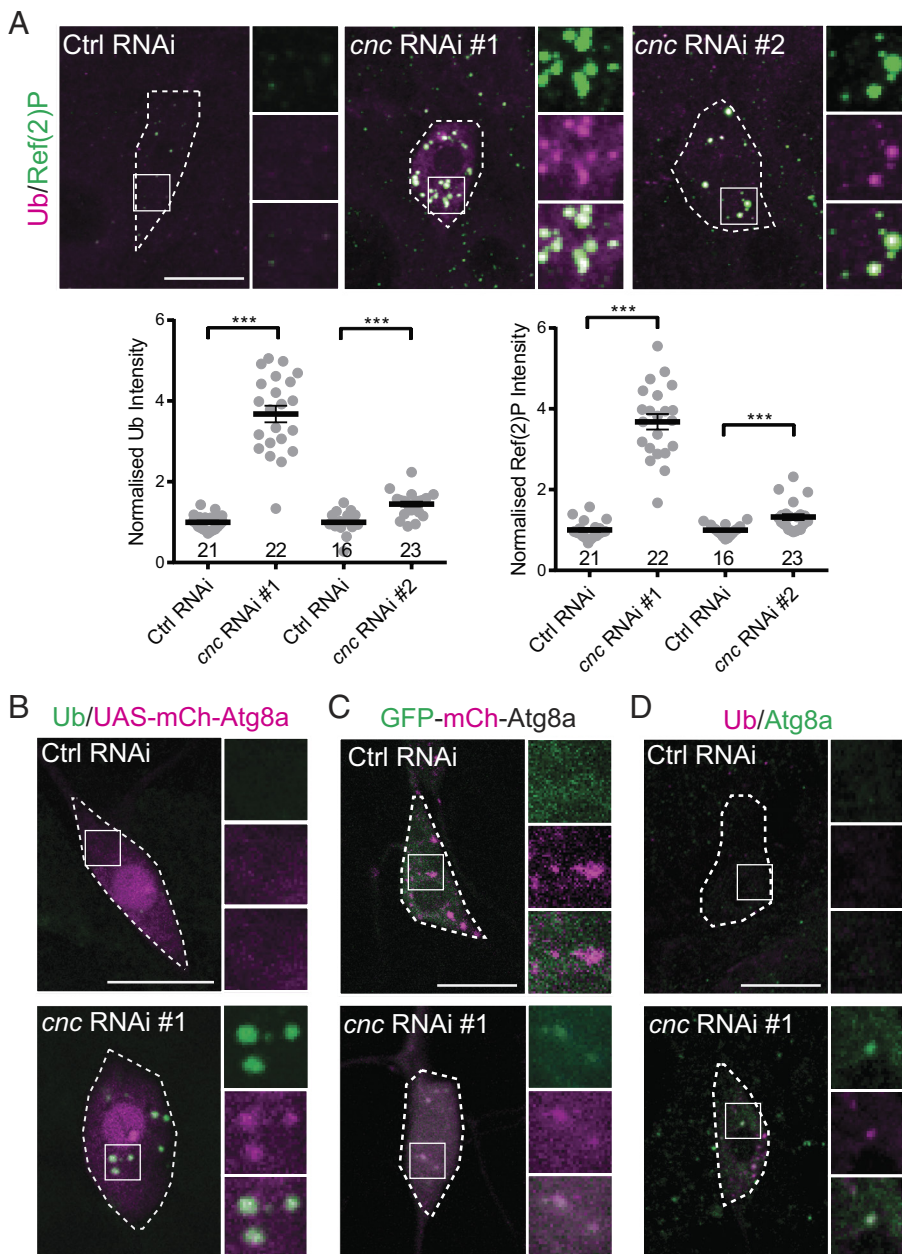


**Fig. 7.** Impaired CncC also resulted in inhibition of autophagy in ddaC neurons. (A) Expression of Ub and Ref(2)P in ddaC neurons expressing control RNAi, *cnc* RNAi #1 or #2. (B) Expression of Ub in control RNAi (n = 26) or *cnc* RNAi #1 (n = 22) ddaC neurons expressing *UAS-mCherry-Atg8a*. (C) Live images of control RNAi (n = 24) or *cnc* RNAi #1 (n = 21) ddaC neurons expressing the GFP-mCherry-Atg8a reporter. (D) Expression of Ub and Atg8a in control RNAi (n = 47) or *cnc* RNAi #1 (n = 58) ddaC neurons. All specimens were observed at the late L3 stage. White dashed lines define the boundary of the ddaC somas. The boxed regions are magnified on the Right panels. Relevant quantifications of normalized Ub and Ref(2)P fluorescent intensities are shown accordingly. Error bars represent  $\pm$  SEM. Two-tailed Student's *t* test (A) was used to determine statistical significance between genotypes (\*\*\**P* < 0.001). The number of neurons (*n*) examined is indicated above the x-axis. The scale bar represent 10  $\mu$ m.

various Atg genes in salivary glands (72). Even though expression of autophagy genes is induced by ecdysone signaling in both remodeling MB  $\gamma$  neurons and salivary glands, the autophagic degradation machinery is dispensable for pruning of MB  $\gamma$  neurons but critical for removal of salivary glands. Thus, the role of autophagy in tissue remodeling is context-dependent during metamorphosis.

Ecdysone signaling downregulates the insulin–TOR pathway via activation of AMPK to control growth and pupal size (73, 74). Both AMPK activation and downregulation of the insulin–TOR pathway are required to induce autophagy in fat bodies (34). Recently, AMPK has been shown to antagonize the insulin–TOR pathway to facilitate dendrite pruning in ddaC neurons (18). We found here that activation of autophagy in ddaC neurons is also mediated by AMPK and repression of insulin–TOR pathway. Loss of AMPK and hyperactivation of the insulin–TOR pathway led to strong accumulation of the Ref(2)P-positive ubiquitinated protein inclusions in ddaC neurons (Fig. 5), resembling those in autophagy-deficient neurons (Fig. 3). Furthermore, the genetic interaction data indicate that AMPK acts upstream to inhibit the insulin–TOR pathway and in turn activate autophagy in ddaC neurons, as suppressing the insulin–TOR pathway rescued the autophagic degradation defects in AMPK-depleted neurons (SI Appendix, Fig. S5 A and B). It is possible that AMPK and insulin–TOR pathway directly regulate autophagy via modulating phosphorylation of the autophagy initiation factor Atg1. In mammals, AMPK has been reported to promote autophagy by directly phosphorylating ULK1/Atg1 or through inhibiting mTOR activity (41). Thus, our study supports the conclusion that in response to ecdysone signaling, autophagy is activated by high AMPK activity and low insulin–TOR pathway in ddaC neurons (SI Appendix, Fig. S10A). Autophagy is thought to mediate the degradation of unwanted proteins to maintain amino acid levels for biosynthesis and energy production during metamorphosis (34). We also found that autophagy-deficient larvae reared on low amino acid diet exhibited more severe pruning defects, suggesting an increased reliance of autophagy on maintaining optimal amino acid levels to facilitate dendrite pruning. In support of it, amino acids have been shown to be an alternative source of energy to power the energy-intensive pruning process (28).

**Autophagy Acts Upstream to Activate CncC Prior to Dendrite Pruning.** Similar to dendrite pruning in fly sensory neurons, mTOR-dependent autophagy is also required for developmental spine pruning in mouse cortical projection neurons. Moreover, hyperactivation of mTOR and impaired autophagy correlate with reduced spine pruning in layer V pyramidal neurons in patients with ASDs (75). However, how autophagy regulates developmental neurite pruning is still unknown. Fly Ref(2)P or its mammalian homolog p62 is able to form a complex with the CncC/Nrf2 inhibitor Keap1. When autophagy is impaired, Ref(2)P/p62 accumulates and sequesters Keap1 into ubiquitinated protein aggregates in mouse livers and adult fly brains, thereby enhancing CncC/Nrf2 activity in flies and mice (22, 52, 54, 61, 62, 76). These studies highlight an inhibitory role of autophagy in CncC/Nrf2, raising a possibility that autophagy might regulate dendrite pruning by suppressing CncC during dendrite pruning. Unexpectedly, multiple lines of evidence demonstrate that autophagy activates CncC to facilitate dendrite pruning in ddaC neurons. First, two readouts of CncC activity, *gstD1-lacZ* and Rpn7, were downregulated upon Atg8a knockdown or depletion (Fig. 6 A and B). Second, Atg8a knockdown also inhibited the nuclear enrichment of CncC protein in ddaC neurons (Fig. 6C). Finally, overexpression or reduction

of CncC suppressed or enhanced the dendrite pruning defects in Atg8a-depleted neurons, respectively (Fig. 6 D and E). In addition, neither endogenous nor overexpressed Keap1 proteins colocalized with those ubiquitin-positive protein aggregates in *Atg8a* RNAi or mutant ddaC neurons (SI Appendix, Fig. S5D), suggesting no sequestration of Keap1 in those autophagy-deficient neurons. Thus, autophagy-dependent regulation of CncC appears to be context-dependent. In ddaC neurons, Atg8a-mediated autophagy regulates dendrite pruning at least partly through activation of CncC. In support of our finding, a recent study has shown that Atg8a-mediated autophagy leads to activation of CncC, rather than suppression, in fly intestines (77).

Since Atg8a can bind to Keap1 in fly and mediate Keap1 degradation in intestines (22), in ddaC neurons Keap1 might be stabilized in the absence of Atg8a, resulting in downregulation of CncC activity. However, Keap1 levels detected by the anti-Keap1 antibody did not differ between *Atg8a* and *keap1* double RNAi neurons and *Atg8a* RNAi controls (SI Appendix, Fig. S11A). Moreover, endogenous Keap1 protein levels, which were detected by *keap1-3 $\times$ FLAG-V5* knock-in line (78), did not alter in *Atg8a* RNAi neurons (SI Appendix, Fig. S11B). Thus, Keap1 does not seem to be degraded through Atg8a-dependent autophagy in ddaC neurons. In addition, *keap1* depletion did not alter the protein levels of the autophagic receptor Ref(2)P, ubiquitinated proteins and the proteasomal subunit Rpn7 (SI Appendix, Fig. S11 C–E), suggesting that Keap1 is not required for CncC-mediated proteasomal degradation and autophagy during dendrite pruning. Therefore, CncC regulates proteasomal degradation and autophagy in ddaC neurons in a Keap1-independent manner. Consistent with our findings, in *Drosophila* S2 cells, CncC appears to control proteasome levels independent of the Nrf2 repressor Keap1 (79).

CncC shows high homology to both Nrf1 and Nrf2 in mammals (23). While Nrf2, antagonized by Keap1, induces antioxidants and detoxifying enzymes upon oxidative stress (20, 23), Nrf1 predominantly promotes proteasomal expression and degradation independent of Keap1 (25, 26, 80). We have recently reported that CncC regulates dendrite pruning through the proteasomal degradation pathway but independent of the antioxidant pathway (18), raising the possibility that CncC functions like Nrf1, instead of Nrf2, in ddaC neurons. Under normal conditions, Nrf1 is an ER-associated glycoprotein which is rapidly degraded by the proteasomes (24). Upon proteasome inhibition or ER stress, Nrf1 is stabilized, deglycosylated by the N-glycanase 1 enzyme Ngly1, and proteolytically cleaved into the active form which enters the nucleus to induce proteasomal subunit expression (24, 81, 82). Interestingly, knockdown of fly Ngly1 led to consistent and severe dendrite pruning defects (SI Appendix, Fig. S12A) as well as robust accumulation of Ref(2)P-positive ubiquitinated protein aggregates (SI Appendix, Fig. S12B), phenocopying *CncC* knockdown. We therefore propose a speculative model showing Keap1-independent and Nrf1-like activation of CncC in ddaC neurons (SI Appendix, Fig. S10B). In wild-type ddaC neurons, CncC, like Nrf1, might be processed by Ngly1 and translocated to the nucleus where it activates proteasomal subunit expression (SI Appendix, Fig. S10B). Impaired autophagy might disrupt CncC processing and/or nuclear enrichment, and thereby inhibit its activation (SI Appendix, Fig. S10C). Future studies are required to investigate how autophagy regulates Nrf1-like activation of CncC during dendrite pruning. Given that the previous studies mostly focused on the Nrf2-like function of CncC, our finding has provided significant insight into the underappreciated Nrf1-like function of CncC in *Drosophila*.

**An Interplay between Autophagy and CncC during Dendrite Pruning.** CncC and Nrf2 have been reported to induce the transcription of both autophagy genes and Ref(2)P/p62 to promote autophagy in flies (fat bodies and intestines) and mammals, respectively (22, 63, 64). CncC and Nrf2 directly bind to the antioxidant response elements of *ref(2)P/p62* to induce their transcriptions in flies and mammals (22, 63). Thus, there exists a feedback loop between autophagy and CncC/Nrf2. We found that in contrast to fat bodies and intestines (22), CncC is dispensable for the expression of Ref(2)P and Atg8a in ddaC neurons. First, overexpression of CncC did not lead to any detectable increase in Atg8a or Ref(2)P expression in ddaC sensory neurons prior to dendrite pruning (*SI Appendix, Fig. S9A*). Moreover, CncC knockdown did not abolish Ref(2)P and Atg8a expression, instead, led to their accumulation on the ubiquitinated aggregates in the mutant neurons (Fig. 7 A and D). Of note, we found that CncC depletion phenocopied *Atg1* and *Atg8a* mutants. First, Ref(2)P-positive protein aggregates formed as punctate structures in these mutant neurons. Second, Atg8a was recruited to the protein aggregates by Ref(2)P in these mutant neurons. Third, the protein aggregates in *cncC* RNAi or *Atg1/8a* RNAi neurons were negative for other early autophagic markers Atg6 and Atg9. Thus, these similar phenotypes suggest that upon CncC depletion, autophagy is impaired in ddaC neurons.

How does CncC regulate autophagy in ddaC neurons? In our previous study, we have demonstrated that CncC induces the expression of various proteasomal subunits in ddaC neurons to enhance proteasomal degradation activity, which is important for dendrite pruning (18). *cncC* depletion impairs the proteasomal degradation machinery and thereby causes undegraded polyubiquitinated proteins, which recruit Ref(2)P to form protein aggregates due to its ubiquitin-binding and self-oligomerizing ability. Atg8a is then recruited by Ref(2)P through their direct interaction to target the protein aggregates for autophagy-mediated clearance. However, the capacity of autophagy-mediated degradation in ddaC neurons appears to be insufficient to clear a considerable amount of ubiquitinated proteins generated upon *cncC* depletion, therefore leading to formation of large Ref(2)P/Atg8a-positive protein aggregates. Studies have demonstrated that compensatory autophagy is strongly upregulated to clear the polyubiquitinated aggregates upon proteasomal dysfunction (58, 83). However, ddaC neurons seem to have an inhibitory mechanism keeping autophagy at a low but indispensable level for cellular homeostasis. In line with this, ddaC sensory neurons have been reported to possess a low level of autophagic activity due to a low expression level of the stress sensor FoxO, compared to strong autophagic activity in epidermal cells (59). Given the low level of autophagy, the ubiquitinated protein aggregates in *cncC* RNAi neurons failed to be cleared through autophagy-dependent degradation, ultimately leading to accumulation of Ref(2)P proteins (Fig. 7A). Endogenous Atg8a was then recruited into the Ref(2)P aggregates (Fig. 7D) through direct interaction (*SI Appendix, Fig. S10D*). Importantly, genetic ablation of the *Atg8a* gene in *cncC* RNAi neurons did not enhance the dendrite pruning defects (*SI Appendix, Fig. S9F*). This suggests that in *cncC* RNAi neurons, Atg8a is largely sequestered by the Ref(2)P-positive protein aggregates.

Therefore, our data strongly suggest that CncC indirectly regulates autophagy activity via proteasomal degradation, representing a mode of autophagic regulation by CncC.

In summary, we show a crucial role of autophagy in regulating protein degradation and dendrite pruning in ddaC neurons. Moreover, autophagy is required for activation of CncC, whereas CncC also affects autophagic activity via proteasomal degradation. Thus, our study indicates an interplay between autophagy and CncC that act interdependently to promote dendrite pruning in sensory neurons.

## Methods

**Fly Strains.** All *Drosophila* stocks were reared on standard laboratory cornmeal diet at 25 °C, unless otherwise stated. Late third instar larvae (110 to 120 h after egg laying) or prepupae at 6, 7, 9, or 16 h APF (both male and female) were used in this study. The details of fly strains and genotypes used in this study are listed in *SI Appendix, Methods*.

**LYD Assays.** Adult males and females were first crossed on the standard laboratory cornmeal diet supplemented with yeast paste for an egg-laying interval of 2 d at 25 °C, and subsequently transferred daily to 1.2% LYD. The ingredients are provided in *SI Appendix, Methods*.

**Live Imaging Analysis of ddaC Sensory Neurons.** Late third instar larvae and prepupae were collected, processed, and imaged using either Olympus FV3000 or Leica TCS SPE2 laser confocal microscopies. The detailed procedures are listed in *SI Appendix, Methods*.

**Immunohistochemistry Assays and Antibodies.** Late third instar larvae and prepupae were dissected and subsequently fixed in 4% formaldehyde for 20 min. The detailed staining procedures and antibody dilutions are listed in *SI Appendix, Methods*.

**Quantification of Immunostaining.** The measurement of fluorescence intensities, the analysis of puncta colocalization, and the quantification of puncta size/number are provided in *SI Appendix, Methods*.

**Statistical Analysis.** Either two-tailed Student's *t* test was used for pairwise comparison, or one-way ANOVA with the Bonferroni test was conducted for multiple-group comparison. See the details in *SI Appendix, Methods*.

**Data, Materials, and Software Availability.** All study data are included in the article and/or *SI Appendix*.

**ACKNOWLEDGMENTS.** We thank E. H. Baehrecke, D. Bohmann, Guang-Chao Chen, H. Eaton, M. Gonzalez-Gaitan, Y. Jan, H. Jasper, A. L. Kolodkin, H. Kramer, J. Terman, T. Uemura, D. Williams, T. K. Kerppola, Bloomington *Drosophila* Stock Center, Developmental Studies Hybridoma Bank (University of Iowa), and Vienna *Drosophila* Resource Center (Austria) for generously providing antibodies and fly stocks. We are grateful to E. H. Baehrecke for helpful discussion. This work was funded by Temasek Life Sciences Laboratory Singapore (TLL-2040).

Author affiliations: <sup>a</sup>Temasek Life Sciences Laboratory, National University of Singapore, Singapore 117604, Singapore; <sup>b</sup>Department of Biological Sciences, National University of Singapore, Singapore 117543, Singapore; <sup>c</sup>Department of Anatomy, Cell and Developmental Biology, Eötvös Loránd University, Budapest H-1117, Hungary; and <sup>d</sup>Institute of Genetics, Biological Research Centre, Szeged H-6726, Hungary

1. M. M. Riccomagno, A. L. Kolodkin, Sculpting neural circuits by axon and dendrite pruning. *Ann. Rev. Cell Dev. Biol.* **31**, 779–805 (2015).
2. L. Luo, D. D. O'Leary, Axon retraction and degeneration in development and disease. *Ann. Rev. Neurosci.* **28**, 127–156 (2005).
3. O. Schuldiner, A. Yaron, Mechanisms of developmental neurite pruning. *Cell. Mol. Life Sci.* **72**, 101–119 (2015).
4. F. Yu, O. Schuldiner, Axon and dendrite pruning in *Drosophila*. *Curr. Opin. Neurobiol.* **27**, 192–198 (2014).

5. D. D. O'Leary, S. E. Koester, Development of projection neuron types, axon pathways, and patterned connections of the mammalian cortex. *Neuron* **10**, 991–1006 (1993).
6. C. R. Keller-Peck *et al.*, Asynchronous synapse elimination in neonatal motor units: Studies using GFP transgenic mice. *Neuron* **31**, 381–394 (2001).
7. T. E. Faust, G. Gunner, D. P. Schafer, Mechanisms governing activity-dependent synaptic pruning in the developing mammalian CNS. *Nat. Rev. Neurosci.* **22**, 657–673 (2021).
8. U. Neniskyte, C. T. Gross, Errant gardeners: Glial-cell-dependent synaptic pruning and neurodevelopmental disorders. *Nat. Rev. Neurosci.* **18**, 658–670 (2017).

9. J. W. Truman, Metamorphosis of the central nervous system of *Drosophila*. *J. Neurobiol.* **21**, 1072–1084 (1990).
10. C. Consoulas, C. Duch, R. J. Bayline, R. B. Levine, Behavioral transformations during metamorphosis: Remodeling of neural and motor systems. *Brain Res. Bull.* **53**, 571–583 (2000).
11. C. T. Kuo, L. Y. Jan, Y. N. Jan, Dendrite-specific remodeling of *Drosophila* sensory neurons requires matrix metalloproteases, ubiquitin-proteasome, and ecdysone signaling. *Proc. Natl. Acad. Sci. U.S.A.* **102**, 15230–15235 (2005).
12. D. W. Williams, J. W. Truman, Remodeling dendrites during insect metamorphosis. *J. Neurobiol.* **64**, 24–33 (2005).
13. D. Kirilly *et al.*, A genetic pathway composed of Sox14 and Mical governs severing of dendrites during pruning. *Nat. Neurosci.* **12**, 1497–1505 (2009).
14. C. Han *et al.*, Epidermal cells are the primary phagocytes in the fragmentation and clearance of degenerating dendrites in *Drosophila*. *Neuron* **81**, 544–560 (2014).
15. C. S. Thummel, Flies on steroids—*Drosophila* metamorphosis and the mechanisms of steroid hormone action. *Trends Genet.* **12**, 306–310 (1996).
16. D. Kirilly *et al.*, Intrinsic epigenetic factors cooperate with the steroid hormone ecdysone to govern dendrite pruning in *Drosophila*. *Neuron* **72**, 86–100 (2011).
17. N. Loncle, D. W. Williams, An interaction screen identifies headcase as a regulator of large-scale pruning. *J. Neurosci.* **32**, 17086–17096 (2012).
18. L. Y. Chew, H. Zhang, J. He, F. Yu, The Nrf2-Keap1 pathway is activated by steroid hormone signaling to govern neuronal remodeling. *Cell Rep.* **36**, 109466 (2021).
19. G. P. Sykiotis, D. Bohmann, Keap1/Nrf2 signaling regulates oxidative stress tolerance and lifespan in *Drosophila*. *Dev. Cell* **14**, 76–85 (2008).
20. H. Motohashi, M. Yamamoto, Nrf2-Keap1 defines a physiologically important stress response mechanism. *Trends Mol. Med.* **10**, 549–557 (2004).
21. G. P. Sykiotis, D. Bohmann, Stress-activated cap'n'collar transcription factors in aging and human disease. *Sci. Signal.* **3**, re3 (2010).
22. A. Jain *et al.*, p62/sequestosome-1, autophagy-related gene 8, and autophagy in *Drosophila* are regulated by nuclear factor erythroid 2-related factor 2 (NRF2), independent of transcription factor TFEB. *J. Biol. Chem.* **290**, 14945–14962 (2015).
23. A. Pitoniak, D. Bohmann, Mechanisms and functions of Nrf2 signaling in *Drosophila*. *Free Radical Biol. Med.* **88**, 302–313 (2015).
24. J. Hamazaki, S. Murata, ER-resident transcription factor Nrf1 regulates proteasome expression and beyond. *Int. J. Mol. Sci.* **21**, 3683 (2020).
25. S. K. Radhakrishnan *et al.*, Transcription factor Nrf1 mediates the proteasome recovery pathway after proteasome inhibition in mammalian cells. *Mol. Cell* **38**, 17–28 (2010).
26. J. Steffen, M. Seeger, A. Koch, E. Krüger, Proteasomal degradation is transcriptionally controlled by TCF11 via an ERAD-dependent feedback loop. *Mol. Cell* **40**, 147–158 (2010).
27. J. J. Wong *et al.*, A Cullin1-based SCF E3 ubiquitin ligase targets the InR/PI3K/TOR pathway to regulate neuronal pruning. *PLoS Biol.* **11**, e1001657 (2013).
28. M. Marzano *et al.*, AMPK adapts metabolism to developmental energy requirement during dendrite pruning in *Drosophila*. *Cell Rep.* **37**, 110024 (2021).
29. L. Yuh Chew, J. He, J. L. Wong, S. Li, F. Yu, AMPK activates the Nrf2-Keap1 pathway to govern dendrite pruning via the insulin pathway in *Drosophila*. *Development* **149**, dev200536 (2022).
30. H. Morishita, N. Mizushima, Diverse cellular roles of autophagy. *Ann. Rev. Cell Dev. Biol.* **35**, 453–475 (2019).
31. D. J. Klionsky *et al.*, Autophagy in major human diseases. *EMBO J.* **40**, e108863 (2021).
32. F. M. Menzies *et al.*, Autophagy and neurodegeneration: Pathogenic mechanisms and therapeutic opportunities. *Neuron* **93**, 1015–1034 (2017).
33. P. Lőrincz, C. Mauvezin, G. Juhász, Exploring autophagy in *Drosophila*. *Cells* **6**, 22 (2017).
34. K. Tracy, E. H. Baehrecke, The role of autophagy in *Drosophila* metamorphosis. *Curr. Top. Dev. Biol.* **103**, 101–125 (2013).
35. A. Bhukel *et al.*, Autophagy within the mushroom body protects from synapse aging in a non-cell autonomous manner. *Nat. Commun.* **10**, 1318 (2019).
36. F. R. Kiral *et al.*, Autophagy-dependent filopodial kinetics restrict synaptic partner choice during *Drosophila* brain wiring. *Nat. Commun.* **11**, 1325 (2020).
37. W. Shen, B. Ganetzky, Autophagy promotes synapse development in *Drosophila*. *J. Cell Biol.* **187**, 71–79 (2009).
38. N. Issman-Zecharya, O. Schuldiner, The PI3K class III complex promotes axon pruning by downregulating a Ptc-derived signal via endosome-lysosomal degradation. *Dev. Cell* **31**, 461–473 (2014).
39. D. F. Egan *et al.*, Phosphorylation of ULK1 (hATG1) by AMP-activated protein kinase connects energy sensing to mitophagy. *Science* **331**, 456–461 (2011).
40. J. Kim, M. Kundu, B. Viollet, K. L. Guan, AMPK and mTOR regulate autophagy through direct phosphorylation of Ulk1. *Nat. Cell Biol.* **13**, 132–141 (2011).
41. M. Zhao, D. J. Klionsky, AMPK-dependent phosphorylation of ULK1 induces autophagy. *Cell Metab.* **13**, 119–120 (2011).
42. K. Piracs *et al.*, Advantages and limitations of different p62-based assays for estimating autophagic activity in *Drosophila*. *PLoS One* **7**, e44214 (2012).
43. R. C. Scott, G. Juhász, T. P. Neufeld, Direct induction of autophagy by Atg1 inhibits cell growth and induces apoptotic cell death. *Curr. Biol.* **17**, 1–11 (2007).
44. K. Hegedűs *et al.*, The Ccz1-Mon1-Rab7 module and Rab5 control distinct steps of autophagy. *Mol. Biol. Cell* **27**, 3132–3142 (2016).
45. N. Mizushima, The ATG conjugation systems in autophagy. *Curr. Opin. Cell Biol.* **63**, 1–10 (2020).
46. A. Jipa *et al.*, Analysis of *Drosophila* Atg8 proteins reveals multiple lipidation-independent roles. *Autophagy* **17**, 2565–2575 (2021).
47. D. N. Martin, E. H. Baehrecke, Caspases function in autophagic programmed cell death in *Drosophila*. *Development* **131**, 275–284 (2004).
48. D. L. Berry, E. H. Baehrecke, Growth arrest and autophagy are required for salivary gland cell degradation in *Drosophila*. *Cell* **131**, 1137–1148 (2007).
49. D. Denton *et al.*, Autophagy, not apoptosis, is essential for midgut cell death in *Drosophila*. *Curr. Biol.* **19**, 1741–1746 (2009).
50. C. T. Kuo, S. Zhu, S. Younger, L. Y. Jan, Y. N. Jan, Identification of E2/E3 ubiquitinating enzymes and caspase activity regulating *Drosophila* sensory neuron dendrite pruning. *Neuron* **51**, 283–290 (2006).
51. D. W. Williams, S. Kondo, A. Krzyzanowska, Y. Hiromi, J. W. Truman, Local caspase activity directs engulfment of dendrites during pruning. *Nat. Neurosci.* **9**, 1234–1236 (2006).
52. M. Komatsu *et al.*, Homeostatic levels of p62 control cytoplasmic inclusion body formation in autophagy-deficient mice. *Cell* **131**, 1149–1163 (2007).
53. I. P. Nezis *et al.*, Ref(2)P, the *Drosophila* melanogaster homologue of mammalian p62, is required for the formation of protein aggregates in adult brain. *J. Cell Biol.* **180**, 1065–1071 (2008).
54. S. Pankiv *et al.*, p62/SQSTM1 binds directly to Atg8/LC3 to facilitate degradation of ubiquitinated protein aggregates by autophagy. *J. Biol. Chem.* **282**, 24131–24145 (2007).
55. I. P. Nezis *et al.*, Cell death during *Drosophila* melanogaster early oogenesis is mediated through autophagy. *Autophagy* **5**, 298–302 (2009).
56. S. Kimura, T. Noda, T. Yoshimori, Dissection of the autophagosome maturation process by a novel reporter protein, tandem fluorescent-tagged LC3. *Autophagy* **3**, 452–460 (2007).
57. I. P. Nezis *et al.*, Autophagic degradation of dBruce controls DNA fragmentation in nurse cells during late *Drosophila* melanogaster oogenesis. *J. Cell Biol.* **190**, 523–531 (2010).
58. P. Löw *et al.*, Impaired proteasomal degradation enhances autophagy via hypoxia signaling in *Drosophila*. *BMC Cell Biol.* **14**, 29 (2013).
59. A. R. Poe *et al.*, Low FoxO expression in *Drosophila* somatosensory neurons protects dendrite growth under nutrient restriction. *Elife* **9**, e53351 (2020).
60. K. Watanabe, Y. Furumizo, T. Usui, Y. Hattori, T. Uemura, Nutrient-dependent increased dendritic arborization of somatosensory neurons. *Genes Cells* **22**, 105–114 (2017).
61. A. Bhattacharjee *et al.*, Loss of ubiquitinated protein autophagy is compensated by persistent cnc1/NFE2L2/Nrf2 antioxidant responses. *Autophagy* **18**, 2385–2396 (2022).
62. M. Komatsu *et al.*, The selective autophagy substrate p62 activates the stress responsive transcription factor Nrf2 through inactivation of Keap1. *Nat. Cell Biol.* **12**, 213–223 (2010).
63. A. Jain *et al.*, p62/SQSTM1 is a target gene for transcription factor NRF2 and creates a positive feedback loop by inducing antioxidant response element-driven gene transcription. *J. Biol. Chem.* **285**, 22576–22591 (2010).
64. M. Pajares *et al.*, Transcription factor NFE2L2/NRF2 is a regulator of macroautophagy genes. *Autophagy* **12**, 1902–1916 (2016).
65. A. K. H. Stavoe, E. L. F. Holzbaur, Autophagy in neurons. *Annu. Rev. Cell Dev. Biol.* **35**, 477–500 (2019).
66. S. B. Dutta, G. A. Linneweber, M. Adriantsilavo, P. R. Hiesinger, B. A. Hassan, EGFR-dependent suppression of synaptic autophagy is required for neuronal circuit development. *Curr. Biol.* **33**, 517–532.e5 (2023).
67. Á. Szabó *et al.*, LC3-associated phagocytosis promotes glial degradation of axon debris after injury in *Drosophila* models. *Nat. Commun.* **14**, 3077 (2023).
68. T. Hara *et al.*, Suppression of basal autophagy in neural cells causes neurodegenerative disease in mice. *Nature* **441**, 885–889 (2006).
69. M. Komatsu *et al.*, Loss of autophagy in the central nervous system causes neurodegeneration in mice. *Nature* **441**, 880–884 (2006).
70. S. Isogai *et al.*, Crystal structure of the ubiquitin-associated (UBA) domain of p62 and its interaction with ubiquitin. *J. Biol. Chem.* **286**, 31864–31874 (2011).
71. I. Alygari *et al.*, Combining developmental and perturbation-seq uncovers transcriptional modules orchestrating neuronal remodeling. *Dev. Cell* **47**, 38–52.e36 (2018).
72. C. Y. Lee *et al.*, Genome-wide analyses of steroid- and radiation-triggered programmed cell death in *Drosophila*. *Curr. Biol.* **13**, 350–357 (2003).
73. J. Colombani *et al.*, Antagonistic actions of ecdysone and insulins determine final size in *Drosophila*. *Science* **310**, 667–670 (2005).
74. C. Mirth, J. W. Truman, L. M. Riddiford, The role of the prothoracic gland in determining critical weight for metamorphosis in *Drosophila melanogaster*. *Curr. Biol.* **15**, 1796–1807 (2005).
75. G. Tang *et al.*, Loss of mTOR-dependent macroautophagy causes autistic-like synaptic pruning deficits. *Neuron* **83**, 1131–1143 (2014).
76. P. Nagy, A. Varga, K. Piracs, K. Hegedűs, G. Juhász, Myc-driven overgrowth requires unfolded protein response-mediated induction of autophagy and antioxidant responses in *Drosophila melanogaster*. *PLoS Genet.* **9**, e1003664 (2013).
77. I. A. Rodriguez-Fernandez, Y. Qi, H. Jasper, Loss of a proteostatic checkpoint in intestinal stem cells contributes to age-related epithelial dysfunction. *Nat. Commun.* **10**, 1050 (2019).
78. R. Wang *et al.*, PINK1, Keap1, and Rtnl1 regulate selective clearance of endoplasmic reticulum during development. *Cell* **186**, 4172–4188.e18 (2023).
79. K. B. Grimberg, A. Beskow, D. Lundin, M. M. Davis, P. Young, Basic leucine zipper protein Cnc-C is a substrate and transcriptional regulator of the *Drosophila* 26S proteasome. *Mol. Cell Biol.* **31**, 897–909 (2011).
80. Y. Zhang, D. H. Crouch, M. Yamamoto, J. D. Hayes, Negative regulation of the Nrf1 transcription factor by its N-terminal domain is independent of Keap1: Nrf1, but not Nrf2, is targeted to the endoplasmic reticulum. *Biochem. J.* **399**, 373–385 (2006).
81. N. J. Lehrbach, G. Ruvkun, Proteasome dysfunction triggers activation of SKN-1A/Nrf1 by the aspartic protease DDI-1. *Elife* **5**, e17721 (2016).
82. F. M. Tomlin *et al.*, Inhibition of NGLY1 inactivates the transcription factor Nrf1 and potentiates proteasome inhibitor cytotoxicity. *ACS Central Sci.* **3**, 1143–1155 (2017).
83. S. Kageyama *et al.*, Proteasome dysfunction activates autophagy and the Keap1-Nrf2 pathway. *J. Biol. Chem.* **289**, 24944–24955 (2014).